Melting and Freezing of Argon in a Granular Packing of Linear Mesopore Arrays

Christof Schaefer, Tommy Hofmann, Dirk Wallacher, Patrick Huber,* and Klaus Knorr†

Faculty of Physics and Mechatronics Engineering, Saarland University, D-66041 Saarbrücken, Germany

(Received 19 December 2007; published 29 April 2008)

Freezing and melting of Ar condensed in a granular packing of template-grown arrays of linear mesopores (SBA-15, mean pore diameter 8 nm) has been studied by specific heat measurements C as a function of fractional filling of the pores. While interfacial melting leads to a single melting peak in C, homogeneous and heterogeneous freezing along with a delayering transition for partial fillings of the pores result in a complex freezing mechanism explainable only by a consideration of regular adsorption sites (in the cylindrical mesopores) and irregular adsorption sites (in niches of the rough external surfaces of the grains and at points of mutual contact of the powder grains). The tensile pressure release upon reaching bulk-liquid–vapor coexistence quantitatively accounts for an upward shift of the melting and freezing temperature observed while overfilling the mesopores.

DOI: 10.1103/PhysRevLett.100.175701 PACS numbers: 64.70.Nd, 65.40.Ba, 65.80.+n

The arguably most conspicuous effect of pore confinement on molecular condensates is the shift of phase transitions with respect to the nonconfined bulk state. Thus condensation (the vapor-liquid transition) does not occur at the saturated vapor pressure p_0 of the bulk liquid but in a wide range of reduced vapor pressures $P = p/p_0$, $P < 1$, starting with the condensation of an adsorbed layer on the pore walls and culminating in pore filling via capillary condensation [1]. In a similar way, melting and freezing of the material in the pores occur at temperatures T well below the bulk triple point temperature T_3 [2]. These reductions are usually interpreted in terms of the Kelvin and the Gibbs-Kelvin equation, respectively. Here interfacial energies are introduced, and, because of their competition with volume free energies, the shift scales with the inverse of the characteristic linear dimension L of the geometric configuration. In the case of tubular pores, this is the pore radius R.

Here we present an experimental calorimetric study on the melting and freezing of one of the most simple condensates imaginable, the rare gas Ar, in a template-grown mesoporous silica known as SBA-15 and considered one of the most ideal mesoporous substrates available [3].

The preparation has been described elsewhere [4]. The material obtained is a powder of grains, about 1 μm in size, which have a relatively rough surface (Fig. 1). The pores within the grains are linear, nonramified, and parallel, have a relatively uniform cross section, and form a periodic 2D hexagonal array. Hence, network effects and the blocking of the solidification front in bottlenecks [5] are not expected to play a major role. The Bragg angles of the diffraction pattern of the empty pore lattice give a lattice parameter (= pore-pore-distance) of 10.7 nm [4]. A fit of a radial electron density $\rho(r)$ profile to the Bragg intensities (with $\rho = 0$ for $r < R_0 - d$ and $\rho =$ constant for $r > R_0 + d$ and with a linear function in the "corona" in between) yields a pore radius R_0 of 3.8 nm, corresponding to a porosity of 0.49, and a corona thickness $2d$ of 2.2 nm. A volumetric Ar sorption isotherm (normalized uptake $f = n/n_0$ as a function of the reduced vapor pressure P, where n is the adsorbed amount of Ar and $n_0 =$ 30 mmol is the amount of Ar for complete filling of the pores), recorded in the liquid regime of the Ar pore filling at 86 K, is shown in Fig. 1. The initial reversible part is due to the condensation of Ar onto the pore walls and the hysteretic part to the filling of the pores by capillary condensation on p increase (starting at about $f_A = 0.65$) and to the evaporation of the capillary condensate on p decrease (terminating at about $f_D = 0.42$). The branches of the hysteresis loop are relatively steep compared to what is observed for other mesoporous substrates, suggesting a narrow distribution of the pore radius and the absence of pore network effects such as pore blocking [6]. The final slope in the postfilling regime $f > 1$ (absent, e.g., for monolithic Vycor substrates) demonstrates that there are further sites available for condensation, with characteristic linear dimensions larger than R_0 but still finite. We think of tapered pore mouths, niches of the rough external surface

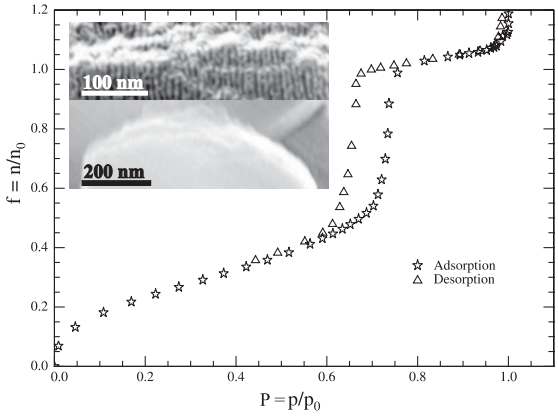

FIG. 1. Ar sorption-isotherm in SBA-15, measured at 86 K. Inset: Scanning electron micrographs of a SBA-15 grain taken with different spatial resolutions as indicated in the figure.

of the grains, and the points at which the powder grains are in mutual contact.

The calorimeter consists of the sample cell, a heat shield, and the outer jacket, with two separate vacuum spaces in between. The sample cell and the heat shield are equipped with thermometers (1000 Ω Pt resistors) and resistance heaters. The heat shield is in thermal contact with the cold plate of a closed cycle He refrigerator.

The cell contains 1.3 g SBA-15 and a coil of Ag wire (that is meant to reduce the thermal time constant within the powder). Twelve fractional fillings have been investigated that have been prepared by introducing suitable amounts of Ar into the cell via a fill line at 86 K.

We employ a scanning experiment where the calorimetric signal is proportional to dQ/dT, the amount of heat per unit T interval that goes into or comes out of the sample. $dQ/dT = K\Delta T/r$, where ΔT and K are the temperature difference and the heat leak between cell and shield, respectively, and r is the cooling and heating rate of the shield. The heat leak has been realized by a He gas pressure of a few millibars in the vacuum space between the cell and the shield, ΔT was typically 1 K, and the heating and cooling rate was held constant at a value of 0.05 K/min. Quite elaborate thermometry allowed us to work with such low rates, which are more than 1 order of magnitude smaller than what is standard with commercial equipment.

The samples have been subject to a complete freezing and heating cycle starting at 86 K in the liquid regime, taking the sample to a minimum temperature of 50 K deep in the solid regime, and bringing it back to 86 K. The results for a selected set of fillings are shown separately for cooling and heating in Fig. 2.

Samples with $f \geq 0.45$ do show heating and freezing anomalies; samples with $f \leq 0.38$ do not. Analogous observations have been made for Ar in Vycor [7]. Thus a phase-transition-like change from the liquid to the crystalline state is basically reserved to the capillary condensed part of the pore filling. The initial ''dead'' fraction of the condensate up to about $f = 0.4$, adsorbed on the pore walls and filling the niches of the corona, does not participate in a collective freezing and melting process.

Melting of the ''mobile'' part occurs in a relatively narrow T interval of 2 K, which for $f < 1$ is centered at 74.5 K, whereas freezing—say, for $f = 0.92$—extends over 7 K from 71.5 K down to 64.5 K with the freezing anomaly having a rather complex shape (Fig. 2). The entropy of fusion S_0 is obtained by integrating the calorimetric signal above the smooth background: $S_0 = c\int(dQ'/dT)/TdT$. The coefficient c has not been determined but is the same for all heating and cooling runs. A plot of S_0 as a function of f is shown in Fig. 3. The values of S_0 obtained from cooling and heating runs are identical within experimental error. This is not only a consistency check but also means that all parts of the freezing anomalies are indeed due to no other phase transition but solidification. For $f < 1$, S_0 is a linear function of f that

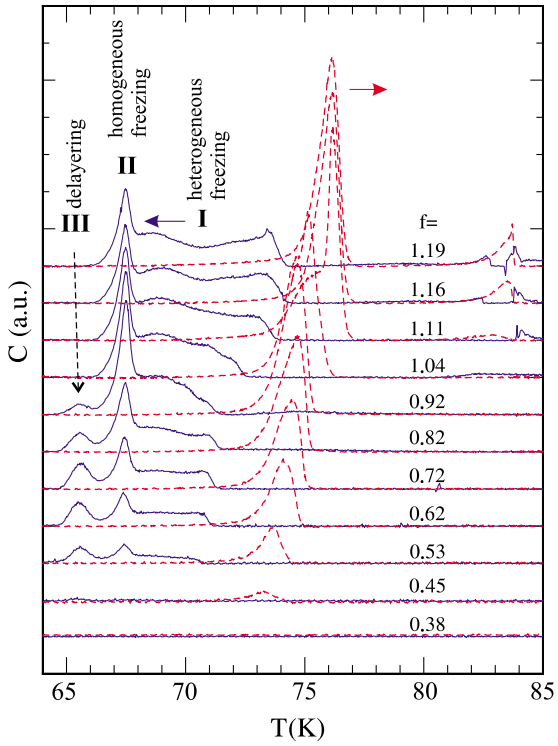

FIG. 2 (color online). Specific heat curves of cooling (solid line) and heating (dashed line) cycles for selected filling fractions f indicated in the figure.

extrapolates to zero at about $f = 0.39$, close to f_D of the 86 K-sorption isotherm. Thus the part of the condensate that supports the collective freezing and melting process comprises not only what is formed by capillary condensation but also the fraction which grows initially in form of a metastable film at the pore walls $(f_A - f_D)$.

For ease of discussion, we divide the freezing anomaly into parts I, II, and III, which are meant to pertain to certain fractions of the pore filling. Parts II and III are the peaks at 67.5 and 65.5 K, respectively, and part I the remainder at higher T. The f dependence of the three parts is also shown in Fig. 3.

The fact that the pore filling solidifies sequentially but melts practically in a single step strongly suggests that solidification leads to a reorganization of the capillary condensate upon which the different fractions I, II, and III of pore material lose their identity.

The melting anomalies have an asymmetric shape. For $f < 1$, the low-T wings of the anomalies for different filling fractions superimpose. We have interpreted the analogous observations on Ar in Vycor in terms of interfacial melting in a cylindrical pore starting at the boundary between the dead and the mobile parts of the pore filling rather than by referring to a pore size distribution which had to be rather special in order to reproduce the peculiar shape of the anomalies [7]. This interfacial melting scenario is similar to surface melting at semiconfined, planar surfaces [8]. Calorimetry can, of course, not prove whether

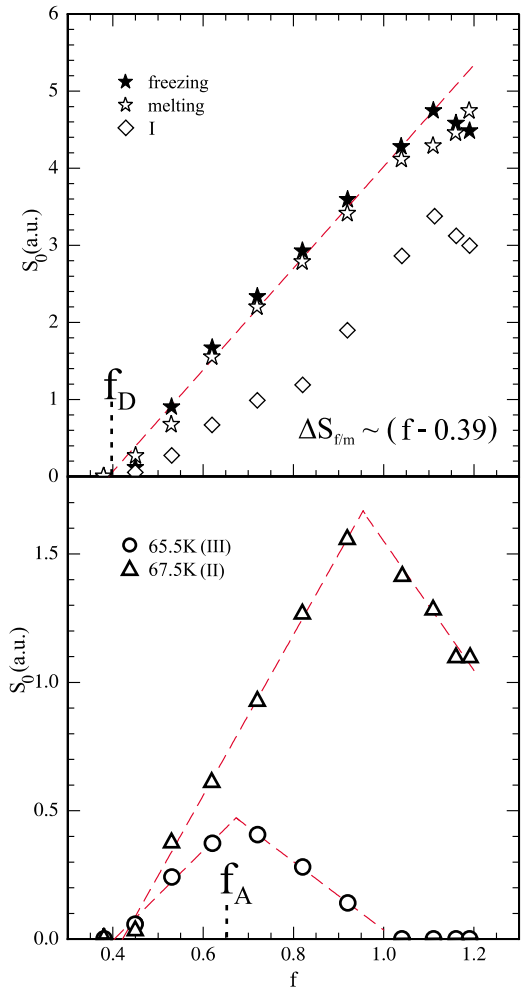

FIG. 3 (color online). Entropy plots of the different anomaly parts as a function of filling fraction f. The dashed lines are guides for the eye.

the melting front propagates along the pores or radially inward, but the mere fact that the asymmetric shape of the anomaly is recovered in the highly homogeneous pores of the present substrate is a strong argument in favor of interfacial, i.e., radial, melting.

As for freezing, part III of the freezing anomaly represents the component of the filling that is the last to solidify on cooling. S_0(III) shows the peculiar type of f dependence, and S_0(III) scales with the vapor-filled fraction of pore space. S_0(III) is due to the solidification of the mobile part of the liquid film on the pore walls in otherwise empty pore segments. Upon solidification, the film delayers, and the material involved joins the already solidified capillary condensate (and melts as such on subsequent heating). The same observations have been made for Ar in Vycor [7].

Still referring to the underfilled situation $f < 1$, this reasoning leaves parts I and II for the freezing of the capillary condensate in the regular pores. We recall that the interfacial melting model not only explains the lowering of the equilibrium freezing and melting temperature T_0 in pore confinement but also predicts metastable states, liquid ones down to the lower spinodal temperature T^- and solid ones up to the upper spinodal temperature T^+. We propose to identify peak II with the freezing of the capillary condensate via homogeneous nucleation of the solid phase at T^-. Peak II is sharp because of the narrow pore size distribution of SBA-15. Part I of the freezing anomaly, on the other hand, stems from the freezing via heterogeneous nucleation within the rather broad (T_0, T^-) interval, triggered by the presence of various types of small nuclei residing at irregular sites. The chance that a parcel of liquid is in contact with such nuclei increases with f. That is why part II dominates (in coexistence with part III) at low f and goes through a maximum slightly below $f = 1$, whereas part I gradually develops with increasing f in a somewhat delayed fashion (Figs. 2 and 3).

The data on the overfilled sample $1.04 < f < 1.19$ shows that the freezing and melting of different parts of the Ar condensate are not independent from each other, an observation that supports the idea of heterogeneous freezing. Quite in contrast to the results on a monolithic Vycor sample, the melting and freezing of the excess material $f - 1$ does not lead to a δ peak at the triple point of the bulk system (at 83.8 K), but in first respect to some extra calorimetric signal at the high-T end of the anomalies, for both freezing and melting. Obviously, most of the excess material resides in sites, say, in niches of the external surface of the powder grains, with dimensions that are still in the nanometer range just slightly larger than the diameter of the regular pores. The presence of this material has an effect on the freezing and melting of the material in the pores. The melting peak for $f = 0.92$, for example, is centered at $T_m = 74.8$ K, but adding excess material to the melting peak eventually shifts to 76.1 K and even reduces the calorimetric signal at the former T_m. Thus, the presence of material outside stabilizes the solid state in the pores.

The pore filling experiences a negative hydrostatic pressure p_h of 70 ± 10 bar for $f < 1$ [9]. This value is dictated by the Laplace equation while assuming semispherical, concave menisci with negative curvature radii of the condensate-vapor interface on the order of the pore radius [10]. Upon postfilling of the pores, the negative curvature of these interfaces gradually vanishes; hence, the tensile pressure in the pore condensate disappears. Based on the p_h dependency of the melting line of Ar [11], an increase of the melting temperature of 1.7 ± 0.3 K is expected for a 70 ± 10 bar pressure release, in good agreement with the $\sim$1.5 K T shift of the melting peak documented in Fig. 2. The upward shift of the onset of the freezing anomaly for $f > 1$ (part I) can be explained in an analogous way. An opposite, downward shift of T_m upon approaching $f = 1$, observed for water in mesopores [12], is consistent with our tensile pressure hypothesis due to water's anomalous $T_m(p_h)$ curve.

For $f = 0.66$, partial cooling and heating cycles have been investigated (Fig. 4). In the first type of such cycles, a part of the condensate is solidified by cooling to some

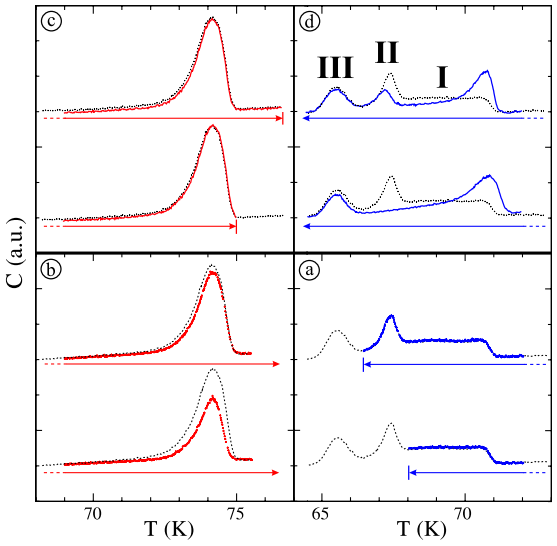

FIG. 4 (color online). Incomplete (partial) cooling-heating cycles at $f = 0.66$ (solid lines) in comparison to heating (cooling) curves after complete solidification (melting) at $f = 0.62$ (dotted lines).

temperature within the T range of the freezing [Fig. 4(a)], and the melting of this part is then studied on subsequent heating [Fig. 4(b)]. In the first run, the freezing of part I is initiated by cooling down to 68 K; in the second one, parts I and II are solidified by cooling down to 66.5 K. As far as position and shape are concerned, the resulting melting anomalies are identical to what is obtained after complete solidification (see Fig. 2 for data on $f = 0.62$ and 0.72); it is just that S_0 is scaled down in proportion to the amount of material solidified on cooling. Parts of the condensate with largely different freezing temperatures melt in the same narrow T interval.

The second type of cycles starts at 60 K deep in the solid regime, and a part of the solid is melted by heating up to temperatures within the T range of melting [Fig. 4(c)]. The resolidification is then studied by subsequent cooling [Fig. 4(d)]. In such partial cycles, the calorimetric signal right at the onset of freezing is enhanced. Obviously, the fraction of material that has been melted in the heating cycle is still in contact with the solid remaining and can therefore resolidify directly without having to overcome a nucleation barrier. Peak III is recovered in the partial cycles. Whenever some part of the pore filling is liquefied, the mobile part of film coating on the pore walls is reestablished. As for peak II, the completed freezing process of the first cooling run down to 60 K leads to a rearrangement of the pore filling in pore space by which the isolated parcels are eliminated, the freezing of which (via homogeneous nucleation) gives rise to peak II. These parcels are not reestablished in the case where melting along the heating run is incomplete. This is why peak II is absent in the lower trace of Fig. 4(d). Even in the case of complete melting by heating to 75.5 K, slightly above the high-T cutoff of the melting anomaly, the isolated parcels are not fully recovered compared to the situation of the virgin sample right after preparation by vapor condensation at 86 K; see the dotted line in Fig. 4. This explains the reduced size of peak II in the upper trace of Fig. 4(d). After a freezing-melting cycle, the pore liquid keeps some memory of the spatial distribution of the pore solid [13].

The freezing-melting phenomenology encountered in SBA-15 challenges the common notion which underlies pore size spectroscopy techniques (“thermoporometry”) [14] relying on simple geometric relations between pore diameter and specific heat anomalies. As demonstrated here, resorting to the specific heat anomaly in neither freezing nor melting will help in a granular packing of mesoporous grains. Freezing is demonstrated to be significantly affected by heterogeneous nucleation, not to mention the delayering transition for partial fillings, whereas melting is governed by interfacial melting processes.

Freezing and melting in such a granular packing of comparably simple linear mesopores is clearly a complicated process. Metastable states, an interplay of homogeneous and heterogeneous nucleation processes, and the coupling between different regions of pore space lead to a remarkable complex phenomenology.

This work has been supported by SFB 277 of the Deutsche Forschungsgemeinschaft.

*p.huber@physik.uni-saarland.de
†knorr@mx.uni-saarland.de

[1] M. W. Cole and W. F. Saam, Phys. Rev. Lett. **32**, 985 (1974).
[2] H. K. Christenson, J. Phys. Condens. Matter **13**, R95 (2001); C. Alba-Simionesco *et al.*, J. Phys. Condens. Matter **18**, R15 (2006); K. Knorr, P. Huber, and D. Wallacher, Z. Phys. Chem. **222**, 257 (2008).
[3] D. Zhao *et al.*, Science **279**, 548 (1998).
[4] T. Hofmann *et al.*, Phys. Rev. B **72**, 064122 (2005); G. A. Zickler *et al.*, *ibid.* **73**, 184109 (2006).
[5] A. Khokhlov *et al.*, New J. Phys. **9**, 272 (2007).
[6] Y. C. Yortsos, *Methods in the Physics of Porous Media* (Academic, New York, 1999).
[7] D. Wallacher and K. Knorr, Phys. Rev. B **63**, 104202 (2001).
[8] D. Zhu and J. G. Dash, Phys. Rev. Lett. **57**, 2959 (1986).
[9] H. Kanda, M. Miyahara, and K. Higashitani, J. Chem. Phys. **120**, 6173 (2004); H. Kanda and M. Miyahara, Adsorption **13**, 191 (2007).
[10] P. Huber and K. Knorr, Phys. Rev. B **60**, 12 657 (1999); J. Hoffmann and P. Nielaba, Phys. Rev. E **67**, 036115 (2003).
[11] A. Michels and C. Prins, Physica (Utrecht) **28**, 101 (1962).
[12] A. Schreiber, I. Ketelsen, and G. H. Findenegg, Phys. Chem. Chem. Phys. **3**, 1185 (2001).
[13] V. P. Soprunyuk, D. Wallacher, P. Huber, K. Knorr, and A. V. Kityk, Phys. Rev. B **67**, 144105 (2003).
[14] M. Brun, A. Lallemand, J. F. Quinson, and C. Eyraud, Thermochim. Acta **21**, 59 (1977).